DOT/FAA/AR-99/8, II

Office of Aviation Research
Washington, D.C. 20591

Improved Barriers to Turbine Engine Fragments: Interim Report II

May 1999

Interim Report

This document is available to the U.S. public through the National Technical Information Service (NTIS), Springfield, Virginia 22161.

U.S. Department of Transportation
Federal Aviation Administration

NOTICE

This document is disseminated under the sponsorship of the U.S. Department of Transportation in the interest of information exchange. The United States Government assumes no liability for the contents or use thereof. The United States Government does not endorse products or manufacturers. Trade or manufacturer's names appear herein solely because they are considered essential to the objective of this report. This document does not constitute FAA certification policy. Consult your local FAA aircraft certification office as to its use.

This report is available at the Federal Aviation Administration William J. Hughes Technical Center's Full-Text Technical Reports page: www.tc.faa.gov/its/act141/reportpage.html in Adobe Acrobat portable document format (PDF).

Technical Report Documentation Page

1. Report No.	2. Government Accession No.	3. Recipient's Catalog No.
DOT/FAA/AR-99/8, II		

4. Title and Subtitle	5. Report Date
IMPROVED BARRIERS TO TURBINE ENGINE FRAGMENTS: INTERIM REPORT II	May 1999
	6. Performing Organization Code
7. Author(s)	8. Performing Organization Report No.
Donald A. Shockey, Jeffrey W. Simons, and David C. Erlich	7412
9. Performing Organization Name and Address	10. Work Unit No. (TRAIS)
SRI International 333 Ravenswood Avenue Menlo Park, CA 94025-3493	11. Contract or Grant No. 95-G-010
12. Sponsoring Agency Name and Address	13. Type of Report and Period Covered
U.S. Department of Transportation Federal Aviation Administration Office of Aviation Research Washington, DC 20591	Interim Report No. 5 29 June through 29 December 1998
	14. Sponsoring Agency Code ANM-100, ANE-100

15. Supplementary Notes

The Federal Aviation Administration William J. Hughes COTR was William Emmerling.

16. Abstract

Because fragments from in-flight engine failures can damage critical aircraft components and produce catastrophic consequences, the Federal Aviation Administration is sponsoring research to mitigate the effects of uncontained engine bursts. SRI International is evaluating the ballistic effectiveness of fabric structures made from advanced polymers and developing a computational ability to design fragment barriers. In this reporting period, SRI solved several numerical problems associated with modeling the crimped geometry and interaction of woven yarns. When an orthotropic model is invoked and direction-dependent yarn properties specified, the yarn, as it is loaded, exhibits no appreciable stiffness until it straightens. The model behaved properly in simple simulations of single yarn response to axial and transverse loads. Laboratory and field site tests were performed to provide data for developing and validating the computational model. The ballistic response of fabrics to fragment impact was evaluated; the phenomenology of fabric deformation and failure was elucidated in quasi-static penetration tests; and the tensile properties of yarns and fibers were measured. Three high-strength polymer materials were examined: PBO (Zylon), aramid (Kevlar), and polyethylene (Spectra). Future work will include verification of the microstructural fabric model by implementing it into the DYNA3D code, simulating the static and dynamic penetration tests, and comparing the results. The material properties most important in resisting penetration will be identified and the effects of boundary conditions investigated. SRI will also perform fragment impact tests to generate data on boundary condition effects, measure yarn-on-yarn friction, and participate in full-scale fragment barrier tests at the Navy Air Warfare Center.

17. Key Words	18. Distribution Statement
Ballistic fabric, Engine fragment, Fragment barrier, High-strength polymers, PBO, Zylon, Aircraft armor, Lightweight armor	This document is available to the public through the National Technical Information Service (NTIS), Springfield, Virginia 22161.

19. Security Classif. (of this report)	20. Security Classif. (of this page)	21. No. of Pages	22. Price
Unclassified	Unclassified	30	

Form DOT F1700.7 (8-72) Reproduction of completed page authorized

TABLE OF CONTENTS

	Page
EXECUTIVE SUMMARY	vii
INTRODUCTION	1
PROGRESS IN EXPERIMENTS	1
Fragment Impact Tests	
Tensile Tests	7
Quasi-Static Penetration (Push) Tests	13
Test Plans	17
PROGRESS IN MODEL DEVELOPMENT	17
Constitutive Model Modification	17
Tests of the Constitutive Model	18
A Single Crimped Yarn Pulled in the Axial Direction	18
A Single Crimped Yarn Loaded Transversely	19
Interaction of Crossing Yarns	20
Transverse Impact of a Crimped Yarn by a Projectile	21
Model Development Plans	22

LIST OF FIGURES

Figure		Page
1	Ballistics Results for a Variety of Materials	3
2	Effect of Weave Tightness	3
3	Effect of Fabric Material	4
4	Effect of Boundary Conditions	4
5	Ballistics Results for Zylon 35 x 35 Fabric	5
6	Ballistics Results from SRI Tests of Zylon Fabric Targets	5
7	Ballistics Results for All Zylon Fabric Tests	6
8	Preliminary Design Curves for Engine Fragment Barriers: Zylon Woven Fabrics Held Firmly on Two Sides	6
9	Tensile Test Results: Fill Yarns From Zylon 30 x 30 Fabric	7
10	Tensile Test Results: Zylon Unwoven Yarn	8
11	Fiber Tensile Tests: Fibers From Unwoven Zylon Yarn	8
12	Fiber Tensile Tests: Fibers From Unwoven Zylon 45 x 45 Warp Yarn	9
13	Fiber From Unwoven Zylon Yarn (After Failure in Fiber Tensile Test)	10
14	Fibers From Woven Kevlar Fabric (After Failure in Yarn Tensile Test)	11
15	Fibers From Woven Spectra Fabric (After Failure in Yarn Tensile Test)	12
16	Push Tests: Effect of Target Material	14
17	Push Tests: Effect of Penetration (Stroke) Rate	14
18	Push Tests: Effect of Boundary Conditions (Gripping)	15
19	Push Tests: Effect of Penetrator Sharpness and Boundary Conditions (Gripping)	15
20	Push Tests: Effect of Overlay on Target Gripped on Four Edges	16
21	Push Tests: Effect of Overlay on Target Gripped on Two Edges	16

22	Finite Element Mesh for a Section of Crimped Yarn	18
23	Stress Developed in Crimped Yarn Under Axial Load	18
24	Calculated Shape of a Single Yarn Loaded in the Axial Direction	19
25	Time History of Effective Stress in a Transversely Loaded Yarn	19
26	Effective Stress for a Single Transversely Loaded Crimped Yarn	20
27	Interaction of Two Crossed Yarns	20
28	Single Yarn Impacted by a Projectile at 80 m/s	21
29	Resisting Force of Yarn Hit by Projectile at 80 m/s	22

EXECUTIVE SUMMARY

Over the years, several civil aircraft accidents with catastrophic consequences have occurred when fragments from in-flight engine failures damaged critical aircraft components. To reduce the probability of such incidents in the future, the Federal Aviation Administration (FAA) is sponsoring research to develop and apply advanced technologies and methods for mitigating the effects of uncontained engine bursts.

In support of this FAA objective, SRI International is conducting a research program to evaluate the ballistic effectiveness of fabric structures made from advanced polymers and to develop a computational ability to design fragment barriers. This semiannual progress report describes the activities and results obtained during the six-month period ending 31 December 1998. Results obtained earlier are reported in previous progress reports.

Since the previous progress report, we have solved several problems associated with the crimped geometry and interaction of woven yarns. When an orthotropic model is invoked and direction-dependent yarn properties are specified, the yarn, as it is loaded, exhibits no appreciable stiffness until it straightens. The calculational behavior of this model was examined in simple simulations of single yarn response to axial and transverse loads and found acceptable.

Laboratory and field site tests were performed to provide data for developing and validating the computational model. We evaluated the ballistic response of fabrics to fragment impact, elucidated the phenomenology of fabric deformation and failure by using quasi-static penetration tests, and measured the tensile properties of yarns and fibers. We focused on three commercially available high-strength polymer materials—PBO (Zylon), aramid (Kevlar), and polyethylene (Spectra).

In future work we will verify the microstructural fabric model by implementing it into the DYNA3D code, simulating the static and dynamic penetration tests, and comparing results. We will also identify the material properties most important in resisting penetration and investigate the effects of boundary conditions. We plan to perform fragment impact tests to generate data on boundary condition effects, measure yarn-on-yarn friction, and participate in full-scale fragment barrier tests at the Navy Air Warfare Center.

INTRODUCTION

Catastrophic civil aircraft accidents have occurred when fragments from in-flight engine failures damaged critical aircraft components. To reduce the probability of such incidents in the future, the Federal Aviation Administration (FAA) is sponsoring research to develop and apply advanced technologies and methods for mitigating the effects of uncontained engine bursts.

In support of this FAA objective, SRI International is conducting a research program to evaluate the ballistic effectiveness of fabric structures made from advanced polymers and to develop a computational ability to design fragment barriers. This semiannual report describes SRIs activities and results during the six-month period ending 31 December 1998. The experiments and computational modeling during this period focused on three commercially available high-strength polymer materials: PBO (Zylon), aramid (Kevlar), and polyethylene (Spectra).

PROGRESS IN EXPERIMENTS

FRAGMENT IMPACT TESTS.

Impact tests were performed at SRI to examine the influence of fabric material, mesh density, boundary conditions (how the fabric is gripped), and impactor sharpness. Impactors included a 25-g (0.055-lb) blunt-edged fragment simulator (FS); a 26-g (0.057-lb) sharp-edged fragment simulator (SFS), whose impact edge more closely resembles that of an actual fan blade; and a larger, 96-g (0.21-lb) blunt-edged fragment simulator (LFS). Impact velocities ranged from 52 to 113 m/s (171 to 371 ft/s), and kinetic energies ranged from 34 to 420 J (25 to 310 ft-lb). The impactors hit approximately end on, with a relatively small pitch and yaw.

Impact tests were also performed at the Navy Air Warfare Center's (NAWC's) 6-in.-bore gas gun facility at China Lake, CA, to examine more realistic, full-scale engine fragment impact scenarios. Impactors for these tests included fan blade and turbine blade fragments from actual aircraft engines, with dimensions up to 13 x 8 x 1 cm (5 x 3 x 0.4 in.) and masses up to 194 g (0.43 lb). Impact velocities ranged from 106 to 210 m/s (349 to 687 ft/s), and kinetic energies ranged from 448 to 4250 J (330 to 3135 ft-lb). The impactors tumbled, so we had no control of the impact orientation.

The target materials included Zylon woven fabrics with meshes ranging from 30 x 30 to 45 x 45 yarns/in. and Kevlar and Spectra woven fabrics with mesh densities of 32 x 32 yarns/in. Target areal densities ranged from 0.013 g/cm^2 (0.027 lb/ft^2) for a single ply of Zylon 30 x 30 to 0.166 g/cm^2 (0.34 lb/ft^2) for nine plies of Zylon 40 x 40.

The tests included several different fabric target boundary conditions. The baseline boundary condition was the target gripped on all four edges. In other tests the target was gripped on only two edges (gripping the ends of the fill yarns, for example, while the ends of the warp yarns remained ungripped) and, for the tests at China Lake, a similar boundary condition was used in which a single long sheet of fabric was continuously wrapped around a rigid frame to form a multiple-ply target.

Figures 1 through 8 illustrate the key results obtained from the impact tests. For the purpose of comparing the ballistic properties of various targets, we define specific energy absorbed (SEA) as the energy absorbed per unit areal density.[1] These results are summarized as follows:

- (Figures 1-3) Zylon woven fabric absorbs significantly more energy per unit areal density (SEA) than any of the other materials tested (nearly twice that of Kevlar or Spectra weaves and over 12 times that of aluminum fuselage skin). Zylon fabrics of different mesh densities have a similar SEA (Zylon 45 x 45 exhibits a slightly higher SEA than the others).

- (Figure 4) Gripping Zylon or Spectra fabric on two edges allows the fabric to absorb significantly more (≈25%-60%) energy than gripping it on four edges (more fabric deformation is able to occur before yarn failure).

- (Figure 5) A sharp-edged impactor penetrates with significantly less energy absorption by the Zylon target than a blunt-edged impactor (yarns fail at lower strains when deformed by a sharp edge). This difference is not as great when the Zylon is gripped on two edges rather than four edges.

- (Figures 6, 7) Tests performed on Zylon fabric targets with the larger impactor (LFS) at SRI and with a variety of impactors at China Lake resulted in SEAs significantly higher (as high as 25,000 J/g/cm^2) than the SEAs obtained in tests with the standard (FS) or sharp-edged (SFS) impactors at SRI (about 2,500 to 3,500 J/g/cm^2). Several factors may enter into this increase:

  - <u>Impactor size and presented impact area</u>—A larger impactor has a larger presented area of impact, so it needs to break more yarns to penetrate. So does an impactor that does not hit end on but instead (like the tumbling impactors in the China Lake tests) hits at various orientations with significant pitch and/or yaw.

  - <u>Fabric target lateral dimensions</u>—A longer yarn absorbs more deformational energy prior to failure than an identical shorter yarn (for most materials, the energy absorbed in a tensile test is proportional to the gage length[2]). Therefore the 12-in.-square targets used in the China Lake tests should absorb more energy than the roughly 6-in.-square targets used in the SRI tests.

  - <u>Number of fabric plies</u>—For multiple-ply targets in which the plies are spaced so that the adjacent plies do not touch each other at any time during the penetration, the energy absorbed would be expected to be proportional to the number of plies. However, the plies in both the SRI and China Lake tests were in close contact, so inter-ply friction and other effects may alter this proportionality.

---

[1]All of the graphs plotting kinetic energy absorbed versus target areal density include, as a reference line, an SEA of 2500 J/g/cm^2 (900 ft-lb/lb/ft^2), which is the value obtained for single-ply targets of Zylon 30 x 30 gripped on four edges and penetrated by the FS at an impact velocity of ≈80 m/s (≈260 ft/s).

[2]For Zylon, there is evidence that the results are not strictly proportional—strain-to-failure increases with decreasing gage length. Nevertheless, the energy absorbed still increases strongly with increasing gage length.

Because there is currently insufficient data concerning the independent variation of these three factors (impactor size, target size, and number of plies) over an adequate range, the influence of each of these factors on the energy absorbed during fragment penetration cannot yet be delineated. Further testing is planned in 1999 to provide more data that will allow for such a determination to be made.

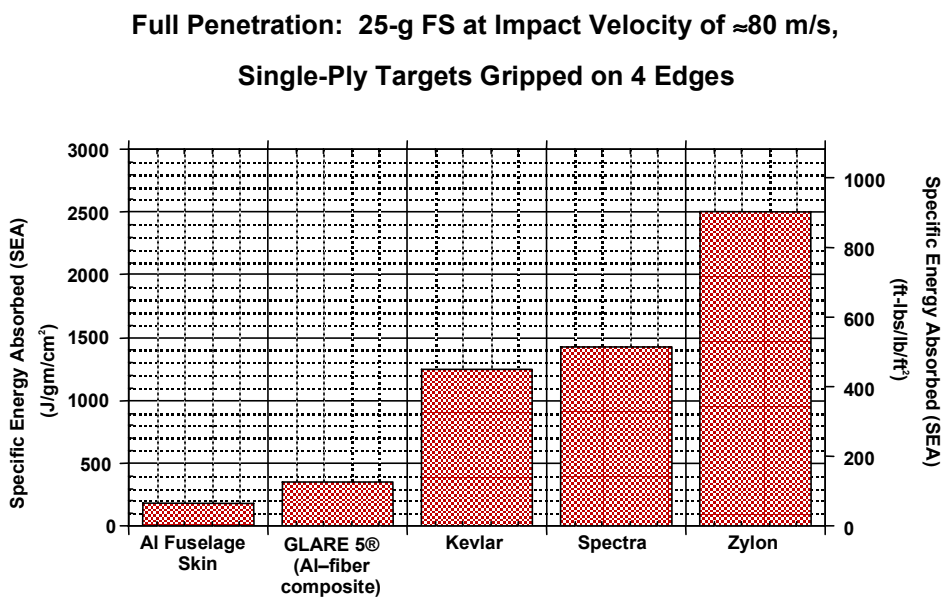

FIGURE 1. BALLISTICS RESULTS FOR A VARIETY OF MATERIALS

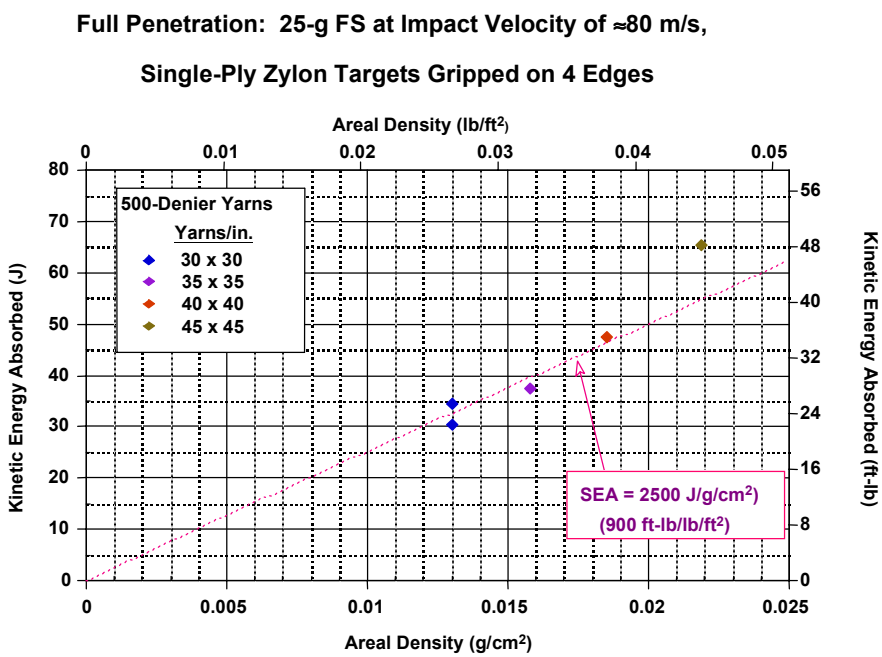

FIGURE 2. EFFECT OF WEAVE TIGHTNESS

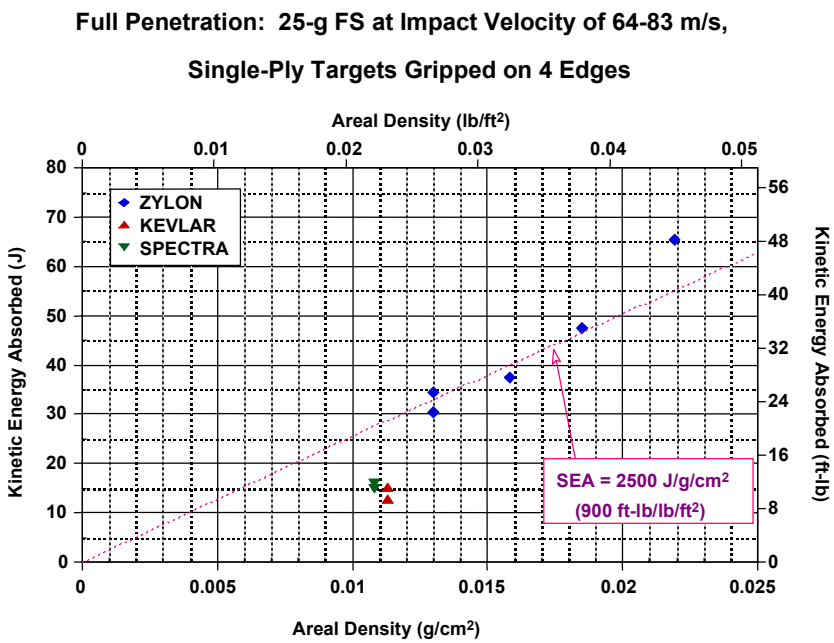

FIGURE 3. EFFECT OF FABRIC MATERIAL

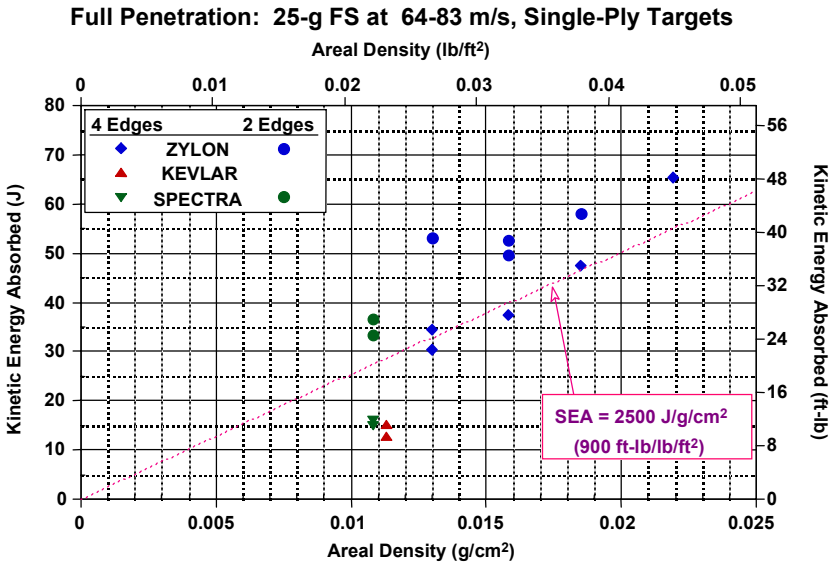

FIGURE 4. EFFECT OF BOUNDARY CONDITIONS

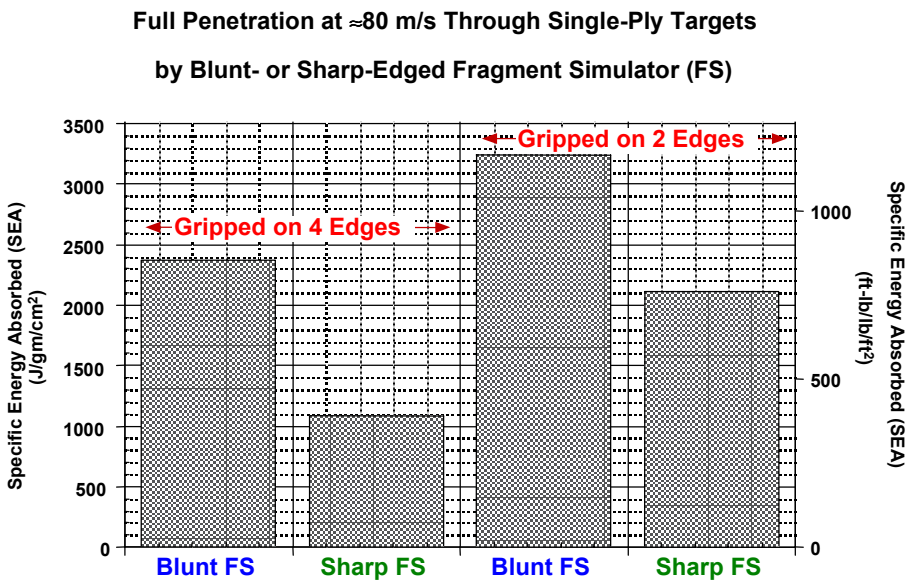

FIGURE 5. BALLISTICS RESULTS FOR ZYLON 35 x 35 FABRIC

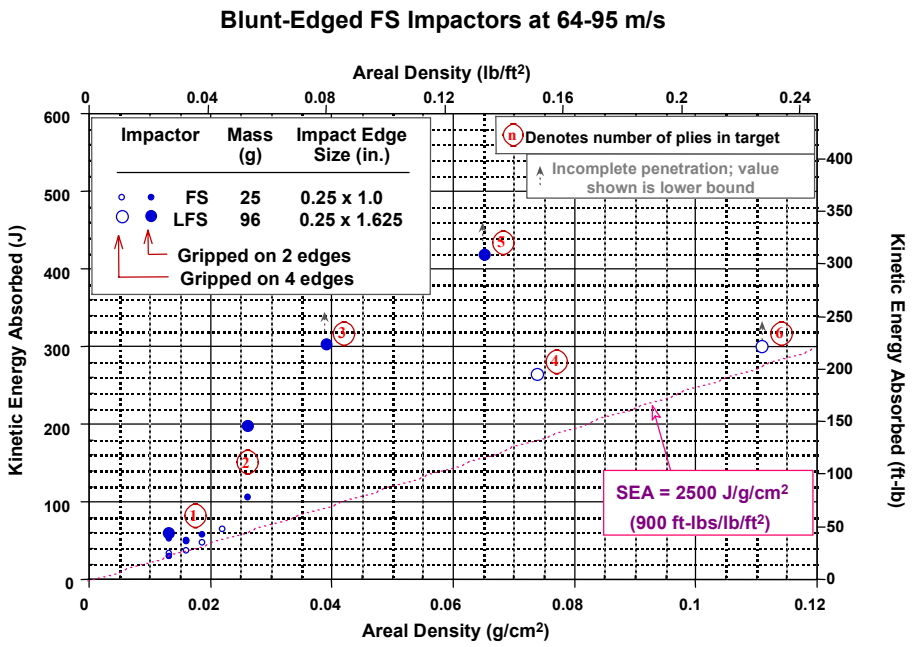

FIGURE 6. BALLISTICS RESULTS FROM SRI TESTS OF ZYLON FABRIC TARGETS

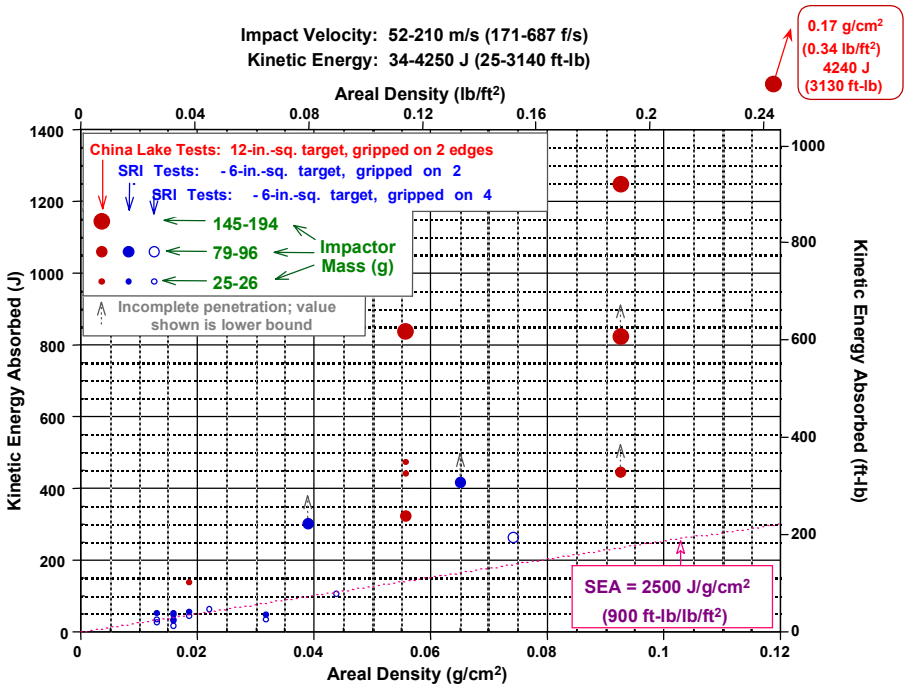

FIGURE 7. BALLISTICS RESULTS FOR ALL ZYLON FABRIC TESTS

However, from the results of the China Lake tests, it can be estimated (figure 8) that a relatively low areal density of Zylon fabric (gripped on two edges)—roughly between 0.15 and 0.25 g/cm^2 (0.3 and 0.5 lb/ft^2)—can stop a relatively large engine fragment (roughly 200 g or nearly 0.5 lb) traveling at a realistic engine fragment exit velocity (slightly more than 200 m/s or nearly 700 ft/s).

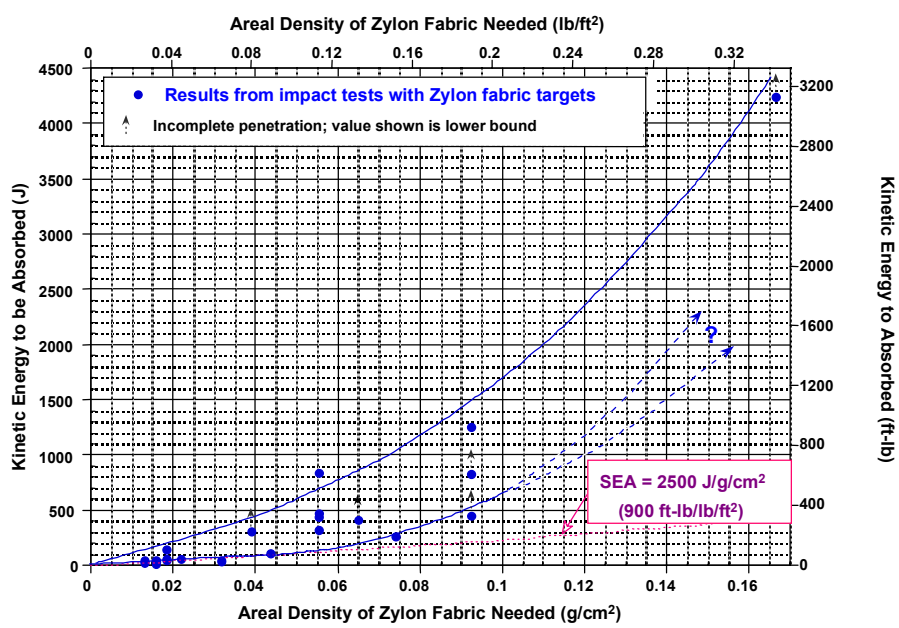

FIGURE 8. PRELIMINARY DESIGN CURVES FOR ENGINE FRAGMENT BARRIERS: ZYLON WOVEN FABRICS HELD FIRMLY ON TWO SIDES

TENSILE TESTS.

In support of computational fabric model development, tensile tests were performed to examine yarn failure phenomenology and to provide material parameters. Test specimens included unwoven Zylon yarn; yarn removed from woven Zylon, Kevlar, and Spectra fabrics; and individual Zylon fibers extracted from the yarn. The tensile tests involved strain rates from 1.6×10^{-3}/s to 15/s and gage lengths from 0.6 to 120 cm (0.25 to 48 in.).

Previous results with Zylon woven yarns showed a small increase in tensile strength and a negligible change in strain-to-failure as a function of strain rate for specimens with the same gage length (figure 9). More recent results, however, show a surprisingly large increase in strain-to-failure and decrease in modulus for shorter gage-length specimens tested at the same strain rate (figure 10). The strains-to-failure obtained for the very shortest (0.6 cm) gage-length specimens were greater than 10%, far higher than the 2.5%-3% observed for the longer gage lengths.

Individual fibers were extracted from both the unwoven Zylon yarn and the woven Zylon 45 x 45 warp yarns (these latter have been crimped more than the yarns in any of the other Zylon fabrics we have examined) and subjected to tensile tests. Just as the yarns did, the individual fibers showed a large decrease in strain-to-failure as a function of gage length (figures 11 and 12). The tests support the theory that weaving damages and weakens the Zylon since fibers from the unwoven yarns had a much larger failure strength than fibers from the woven yarns. Further testing is needed to understand and characterize the effect of gage length variation on the tensile deformation and failure properties.

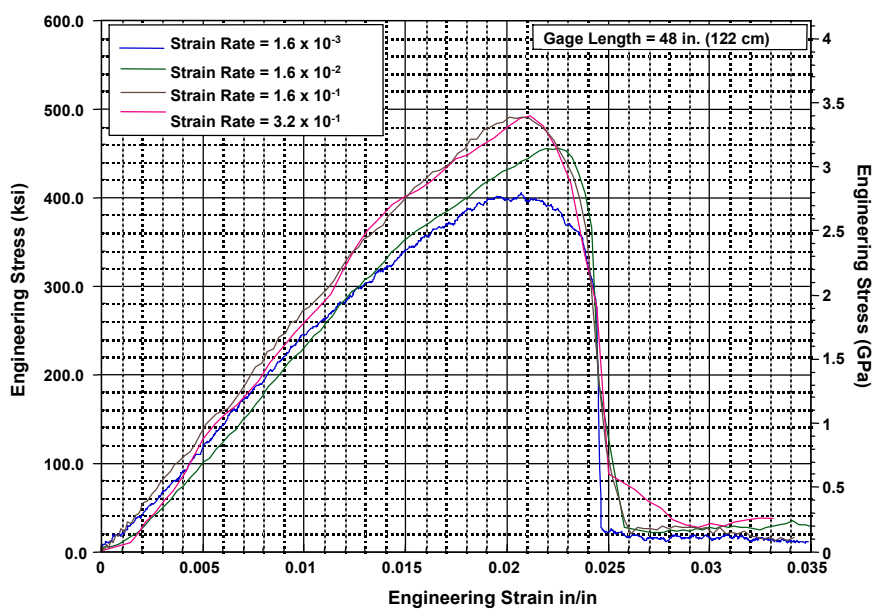

FIGURE 9. TENSILE TESTS RESULTS: FILL YARNS FROM ZYLON 30 x 30 FABRIC

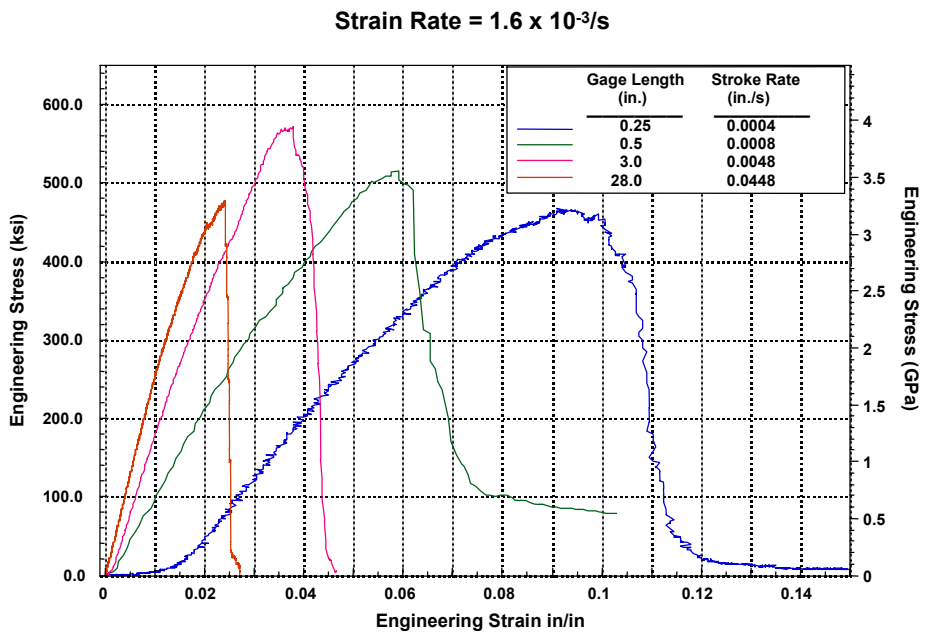

FIGURE 10. TENSILE TEST RESULTS: ZYLON UNWOVEN YARN

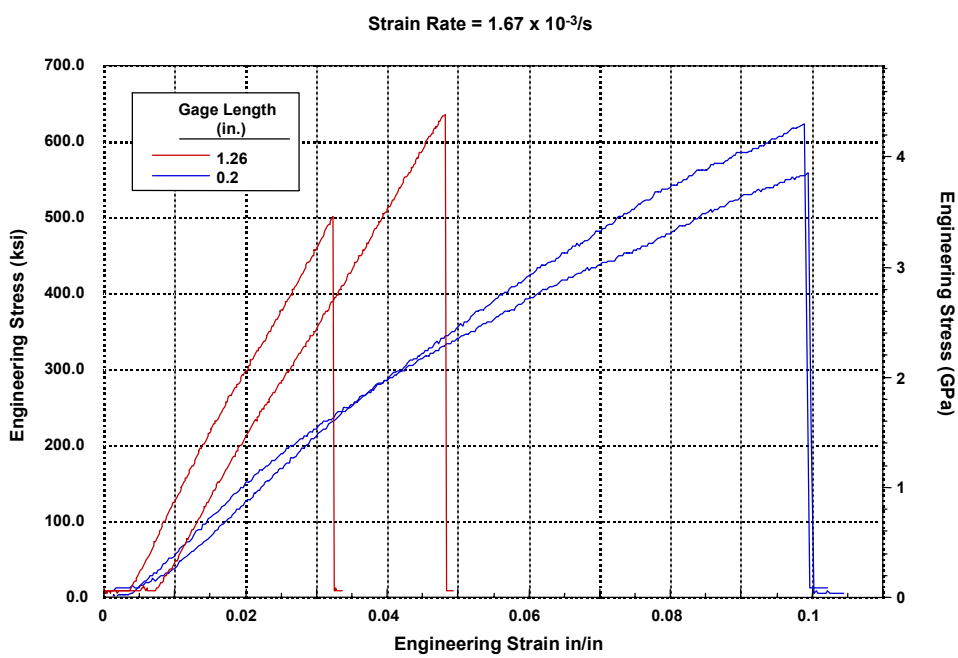

FIGURE 11. FIBER TENSILE TESTS: FIBERS FROM UNWOVEN ZYLON YARN

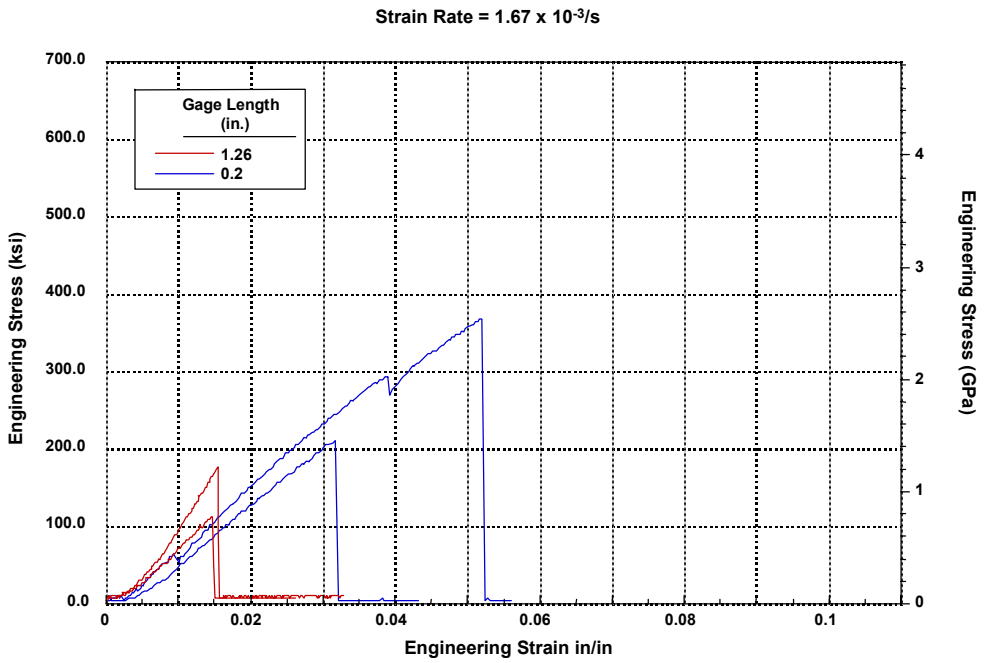

FIGURE 12. FIBER TENSILE TESTS: FIBERS FROM ZYLON 45 x 45 WARP YARN

An examination was made of the structure and failure phenomenology of the high-strength fabric materials. Scanning electron microscopy (SEM) photos of Zylon yarns revealed that they are composed of smooth-walled cylindrical fibers about 13.5 µm in diameter (roughly 250 fibers comprise one 500-denier yarn). Examination of the broken ends of fibers from the tensile tests revealed that each fiber is composed of long, thin microfibrils oriented parallel to the fiber axis.[3] Upon tensile failure, the fiber separates into clumps of these microfibrils, which fail at different distances along the axis (figure 13). Kevlar appears to have a similar structure, with the fibers splitting into microfibrils (or clumps) upon tensile failure (figure 14). Spectra differs in that the ends of its broken fibers are amorphous lumps larger in diameter than the fiber itself and there is little evidence of microfibril breakup[4] (figure 15).

[3]The manufacturer (Toyobo Co., Ltd.) depicts these microfibrils as between 10 and 50 nm in diameter, of unknown length, and with occasional microvoids (elongated in the axial direction) at the microfibril interstices.

[4]This may be caused by the sizing, which is present in the Spectra fabric but not in the Kevlar or Zylon fabrics.

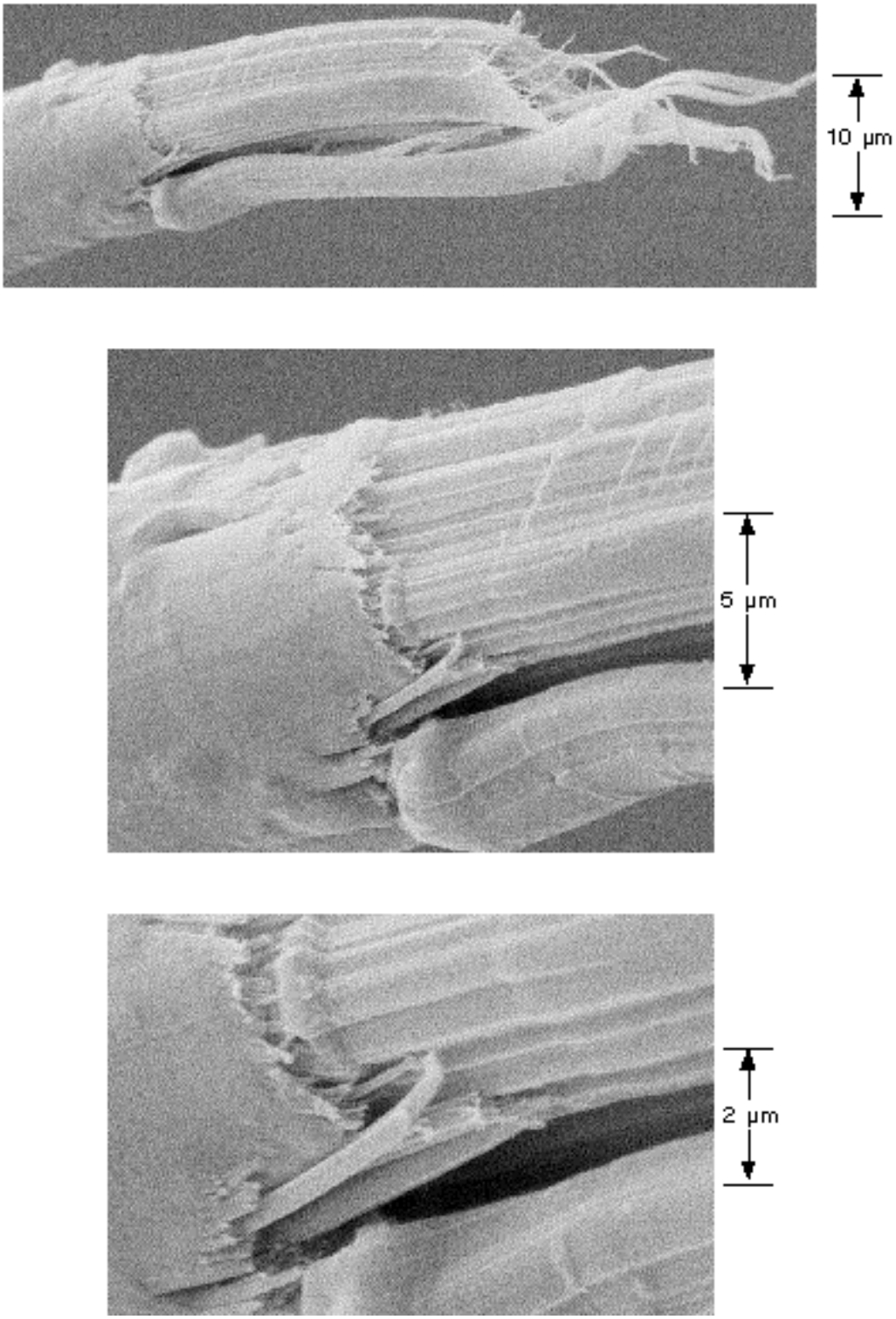

FIGURE 13. FIBER FROM UNWOVEN ZYLON YARN
(AFTER FAILURE IN FIBER TENSILE TEST)

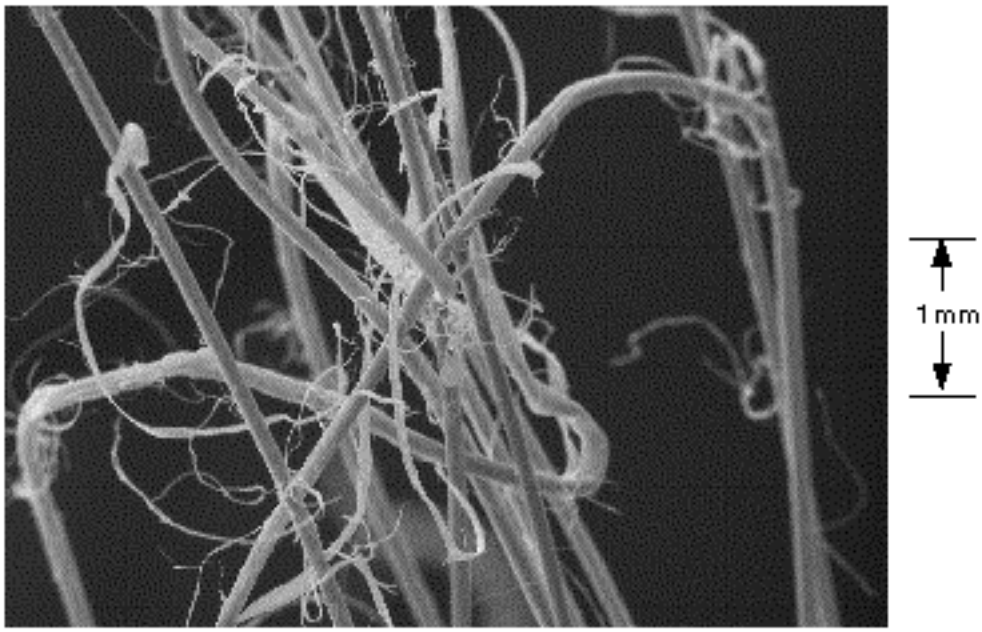

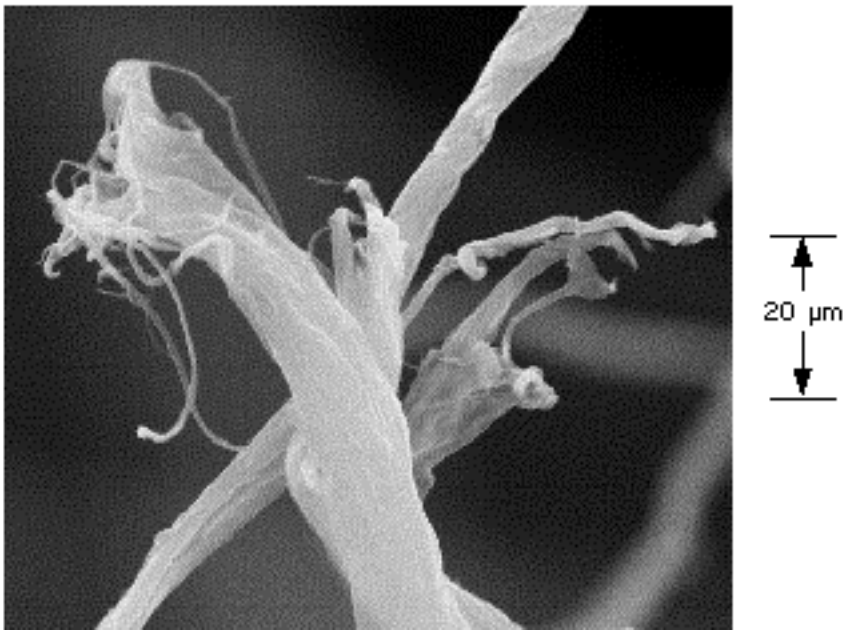

FIGURE 14. FIBERS FROM WOVEN KEVLAR FABRIC
(AFTER FAILURE IN YARN TENSILE TEST)

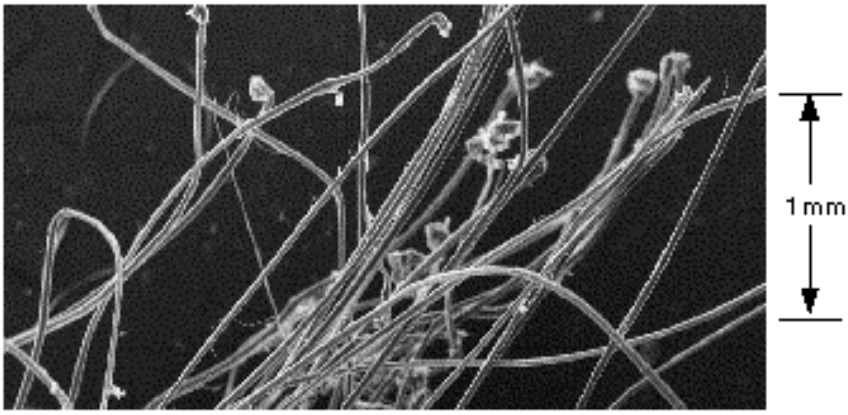

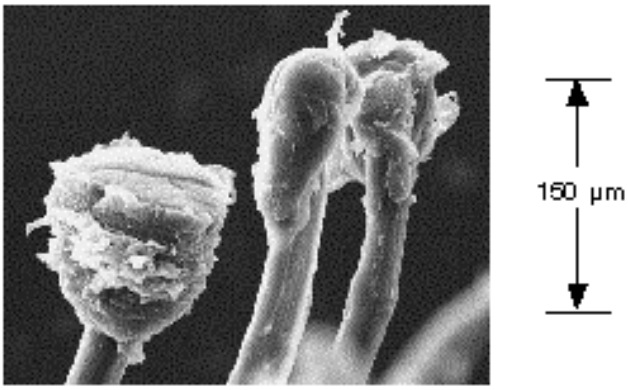

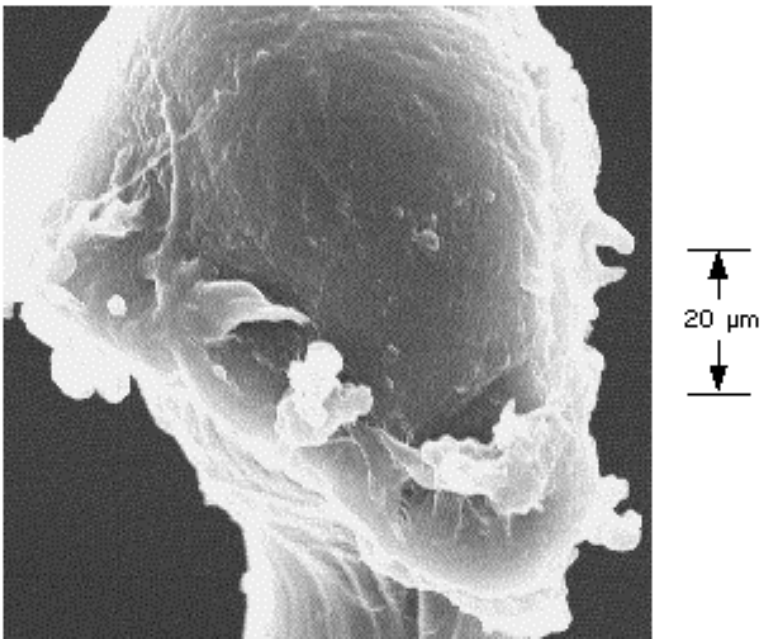

FIGURE 15. FIBERS FROM WOVEN SPECTRA FABRIC
(AFTER FAILURE IN YARN TENSILE TEST)

QUASI-STATIC PENETRATION (PUSH) TESTS.

A series of experiments were performed in which a penetrator was slowly pushed into and through a Zylon target. The load and deflection histories were recorded and the target deformation and failure evolution were videotaped. The features on the recorded load history can be correlated with the observed deformation and failure phenomena (i.e., large sudden drops in load correlate with nearly simultaneous multiple yarn failures while gradual decreases in load correlate with yarn pullout), and the energy absorbed by the target during penetration can be determined by integrating the load-deflection curve. The purposes of these tests were to provide an understanding of the evolution and phenomenology of fabric target deformation and failure, act as a guide model development, and to provide experimental data that can be used for model validation.

Figures 16 through 21 illustrate key results (in terms of the load-deflection curves, total energy absorbed, and SEA) from push tests in which the following test parameters were varied:

- (Figure 16) Target material and mesh density—Zylon 30 x 30 through 40 x 40, Spectra 32 x 32, and Kevlar 32 x 32. SEA for Zylon increases with increasing mesh density. Spectra has a similar SEA to that of the lower-density Zylon meshes, but Kevlar's SEA is significantly lower.

- (Figure 17) Penetrator deflection rate—From ≈ 0.02 to ≈ 20 cm/s (0.0075 to 7.5 in./s). The SEA for Zylon increases somewhat with increasing strain rate.

- (Figure 18) Target boundary conditions—Gripped on two edges and four edges. Although the peak loads are higher for Zylon targets gripped on four edges, the SEA is significantly higher for targets gripped on two edges.

- (Figure 19) Penetrator sharpness—Blunt-edged FS and an actual fan blade (FB). The SEA is far lower for the sharp FB than for the FS (lower by a factor of 6 when the target is gripped on four edges and nearly a factor of 4 lower when the target is gripped on two edges). However, when an FB impacts a target that has an additional ungripped ply of the fabric placed in front of the gripped ply (i.e., as an overlay), the SEA increases dramatically for both four-edge and two-edge gripping (figures 20 and 21). The FB does not penetrate the overlay. Instead the overlay fabric wraps itself around the FB, and both penetrate the gripped target ply (a similar phenomenology was observed for impact tests). The higher SEA is likely caused by the decreased penetrator sharpness and increased impact area resulting from the wrapping.

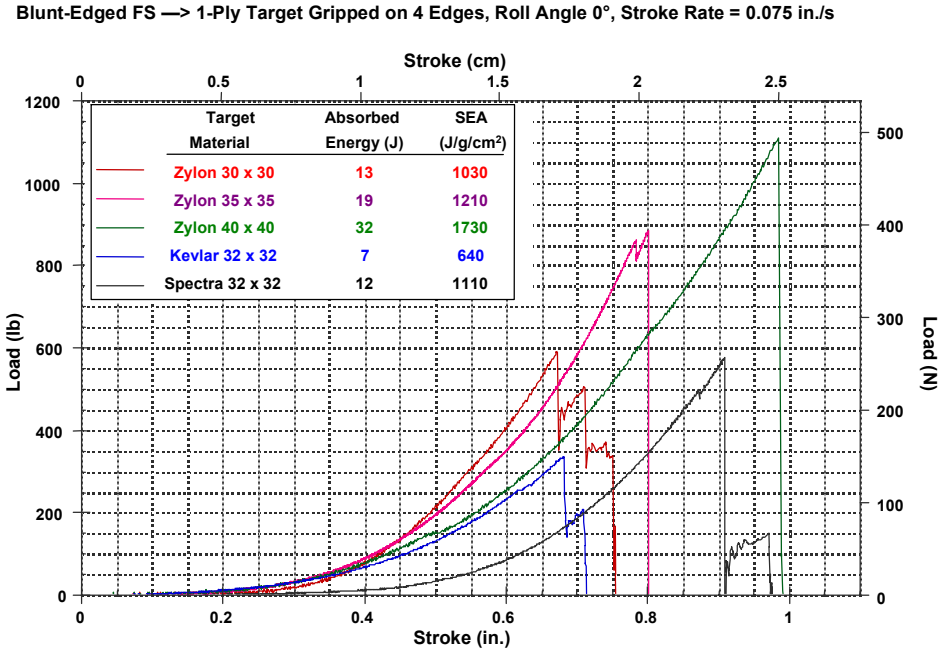

FIGURE 16. PUSH TESTS: EFFECT OF TARGET MATERIAL

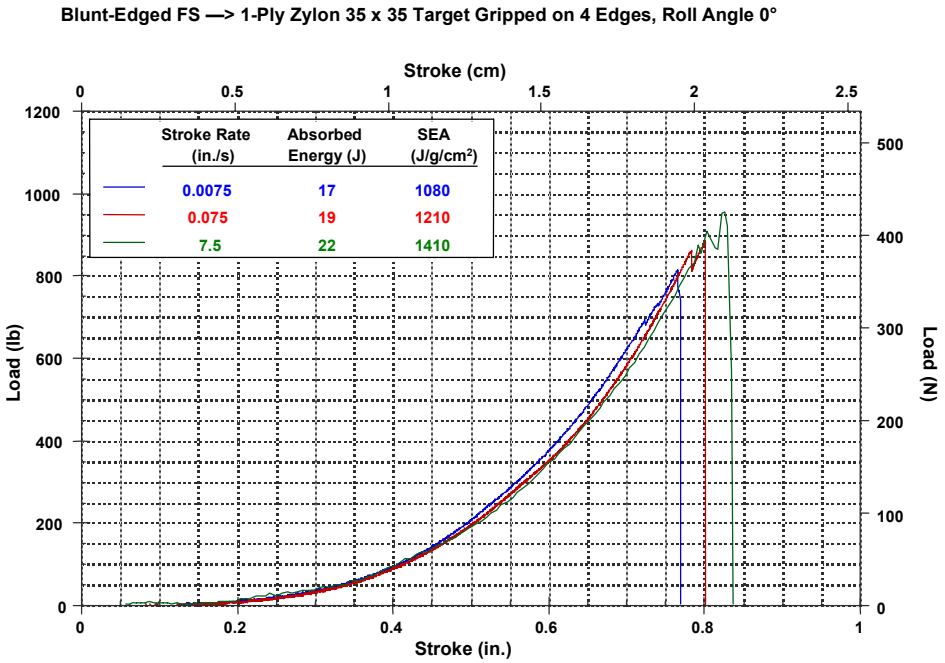

FIGURE 17. PUSH TESTS: EFFECT OF PENETRATION (STROKE) RATE

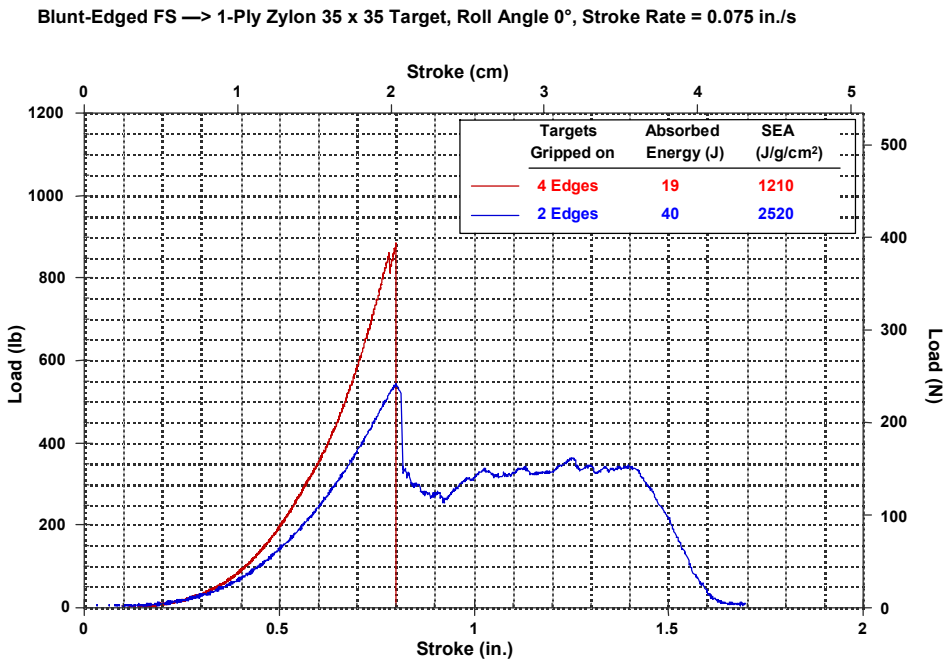

FIGURE 18. PUSH TESTS: EFFECT OF BOUNDARY CONDITIONS (GRIPPING)

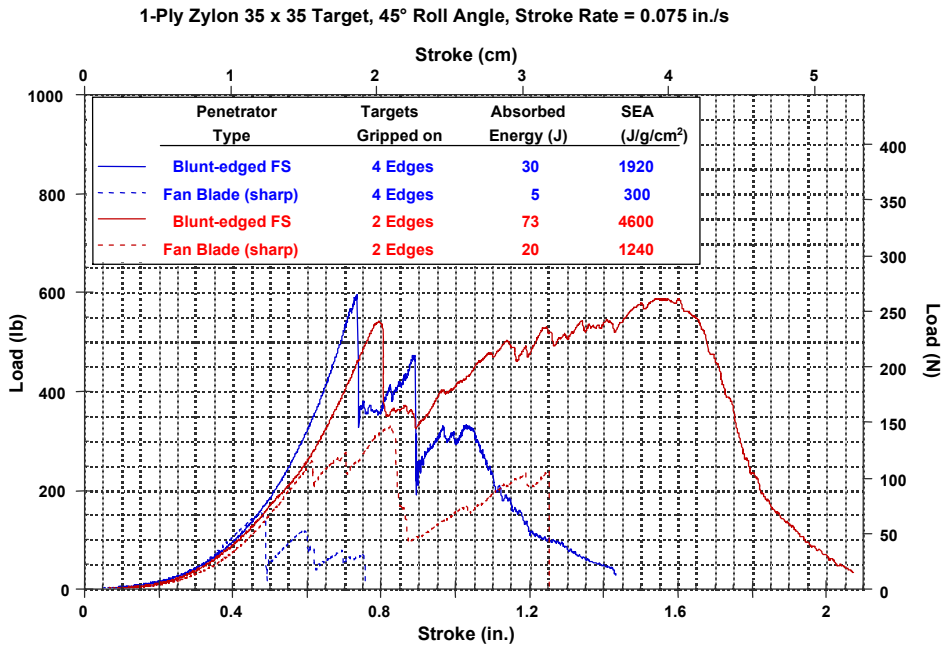

FIGURE 19. PUSH TESTS: EFFECT OF PENETRATOR SHARPNESS AND BOUNDARY CONDITIONS (GRIPPING)

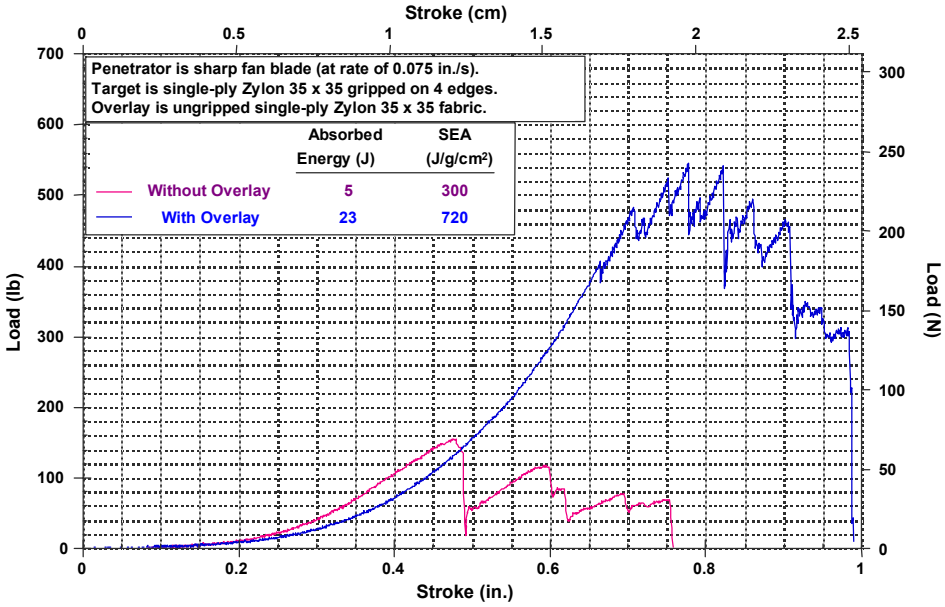

FIGURE 20. PUSH TESTS: EFFECT OF OVERLAY ON TARGET GRIPPED ON FOUR EDGES

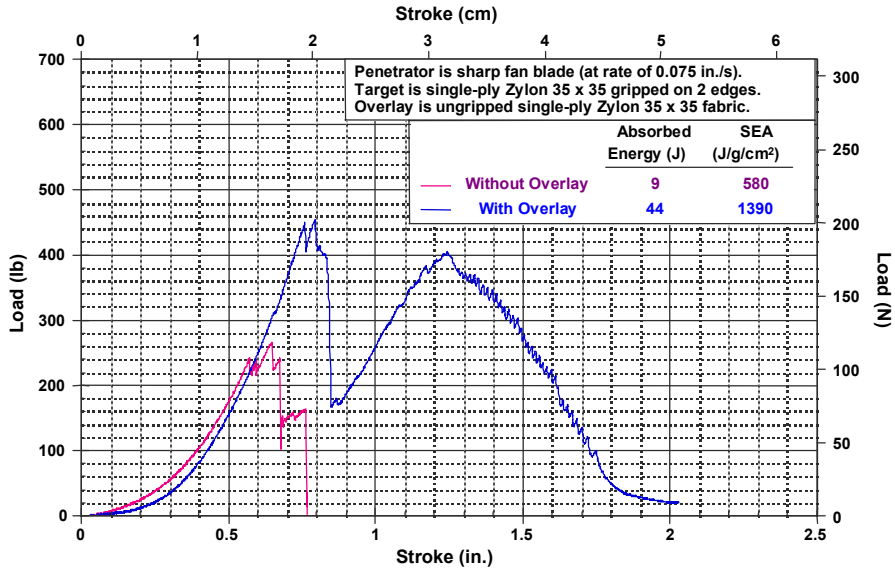

FIGURE 21. PUSH TESTS: EFFECT OF OVERLAY ON TARGET GRIPPED ON TWO EDGES

TEST PLANS.

The following experiments are planned for the remainder of the program:

- Four-inch-bore gas gun tests on small (≈ 6 x 6 in.) targets (15-20 tests): The objective will be to fill in gaps in ballistic data and to try out new configurations (i.e., gluing around edge of interior wall panel, etc.).

- Full-scale tests at China Lake using actual 727 fuselage sections (10-12 tests): In these tests, various practical gripping arrangements for incorporating fabric barriers into existing planes (using existing hardware, i.e., fasteners) will be used and a determination made of which of these arrangements will best utilize the fabric's ballistic strengths.

- Full-scale tests with a 6-in.-bore gas gun at the SRI remote test site (20-30 tests): This series of tests will use the most advantageous designs, as determined from the China Lake tests, and varying impactor and fabric parameters to obtain complete sets of data for modeling.

- Yarn pullout tests (5-10 tests): These tests will measure the force required to pull a single yarn out of a fabric gripped with a known lateral force to provide frictional parameters for fabric modeling.

- Push tests (5-10 tests): The objective of these tests will be to measure force deflection curves for pushing a penetrator through a fabric target, while measuring the lateral force on the target, to provide data on minimum grip strength for designing barriers and for fabric model validation.

- Yarn tensile tests (10-20 tests): The goal of these tests will be to examine the observed variation in the tensile flow curve as a function of gage length observed in previous yarn tensile tests. Modifications to the tests will be made to allow direct measurement of the strain at various locations along the yarn.

PROGRESS IN MODEL DEVELOPMENT

CONSTITUTIVE MODEL MODIFICATION.

The previous progress report showed results with yarns modeled as linear elastic or elastic-plastic. Elastic and elastic-plastic models miss an important characteristic of the yarn response: a crimped yarn does not have any appreciable stiffness until it straightens out. This characteristic results from the yarn being made up of many fibers that easily bend independently when the yarn is straightened out, and it effectively gives the yarn a very low shear modulus. To obtain a continuum treatment of this feature, an orthotropic model was used which allows for definition of an independent Young's modulus, Poisson's ratio, and shear modulus in each of three coordinate directions. In DYNA3D, this is Material Model Number 2. A procedure for damage growth and failure was also implemented into this material model.

TESTS OF THE CONSTITUTIVE MODEL.

The calculational behavior of this model was tested by performing several simple simulations: a single crimped yarn pulled axially, a single crimped yarn loaded transversely, interaction between two intersecting yarns, and a single yarn hit by a projectile.

A SINGLE CRIMPED YARN PULLED IN THE AXIAL DIRECTION. The first simulation was for a single crimped yarn pulled in the axial direction. Figure 22 shows the finite element mesh for a short section of a yarn. The mesh is constructed of solid elements, with eight elements in the cross section. The cross-sectional geometry is modeled to match photographs taken of a yarn cross section. The amount of kink is representative of that found in Zylon yarns in a 30 x 30 pitch fabric weave.

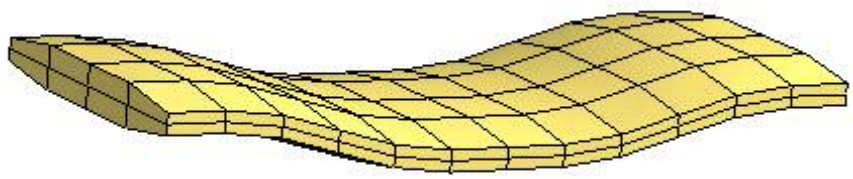

FIGURE 22. FINITE ELEMENT MESH FOR A SECTION OF CRIMPED YARN

The left end of the yarn was pulled at 20 m/s and the right end was held. Figure 23 shows the stress developed in the yarn as it is pulled, and figure 24 shows the shape of the yarn as it straightens out. The stress in the yarn is small initially and increases as the yarn is straightened out. The stress reaches a peak of about 30 kb and then the yarn breaks.

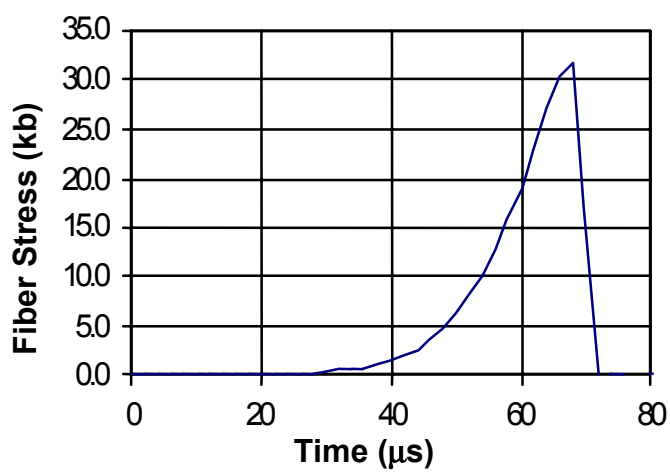

FIGURE 23. STRESS DEVELOPED IN CRIMPED YARN UNDER AXIAL LOAD

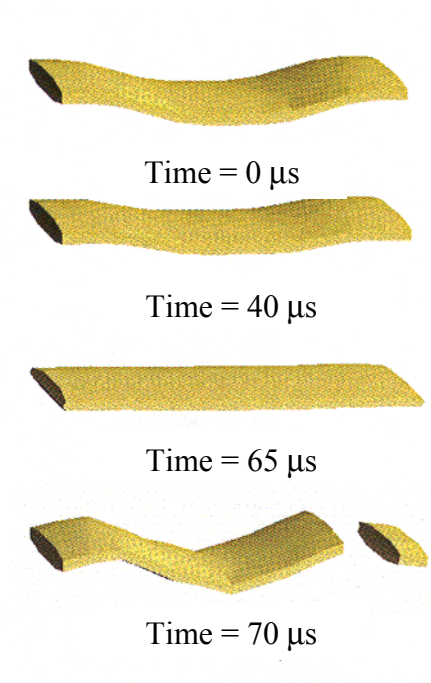

FIGURE 24. CALCULATED SHAPE OF A SINGLE YARN LOADED IN THE AXIAL DIRECTION

A SINGLE CRIMPED YARN LOADED TRANSVERSELY. For the second simulation, the left end of a crimped yarn was displaced transversely at 20 m/s while holding the right end fixed. This example requires that the model undergo large displacements and rotations, as well as stretching, without developing any appreciable resisting load. The calculated resisting stress developed in the yarn is shown in figure 25. The peak stress reached is just above 30 kb. The shape of the yarn as it deforms is shown in figure 26 along with fringes of effective stress in the yarn.

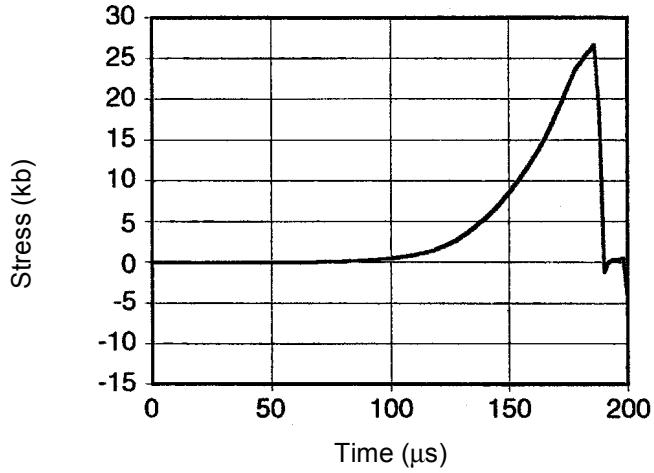

FIGURE 25. TIME HISTORY OF EFFECTIVE STRESS IN A TRANSVERSELY LOADED YARN

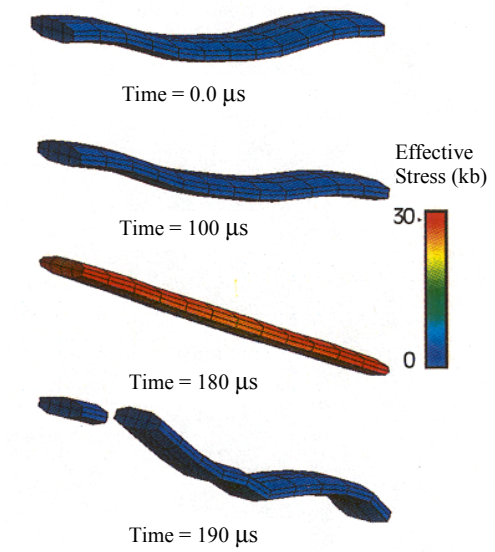

FIGURE 26. EFFECTIVE STRESS FOR A SINGLE TRANSVERSELY LOADED CRIMPED YARN

INTERACTION OF CROSSING YARNS. The third example tests the model for calculating interaction between crossing yarns. This example simulates the interaction between two half-inch-long yarns oriented at 90 degrees to each other and crossing at their centers. As shown in figure 27, the left end of the lower yarn section (shown in yellow) is displaced vertically upward at 80 m/s. As the yellow yarn straightens, it lifts the crossing yarn (green). By 380 µs, the yellow yarn is straight and the green yarn is draped over it. At 400 µs, the yellow yarn breaks.

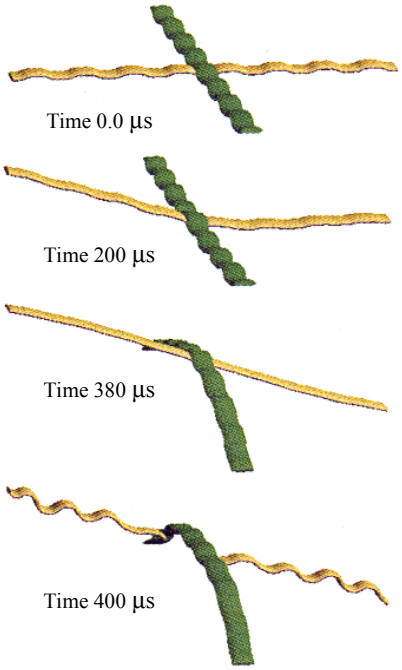

FIGURE 27. INTERACTION OF TWO CROSSED YARNS

TRANSVERSE IMPACT OF A CRIMPED YARN BY A PROJECTILE. The fourth example was to test the capabilities of modeling the interaction between a projectile and a Zylon yarn. This example simulates a single yarn being impacted by a small titanium projectile at 80 m/s. The finite element model is shown in figure 28 at time t = 0.0. Also shown are the response of the impacted yarn and the calculated effective stress in the yarn at various times after impact. At 15 m/s, the deformation in the yarn is moving out from the end of the impactor. Based on the speed of the projectile (80 m/s), the displacement wave in the yarn was estimated to be only about 320 m/s which is much less than the sound speed in a taut yarn (about 14,000 m/s based on elastic properties). At 38 μs the yarn is stretched out, and at 40 μs the yarn is broken.

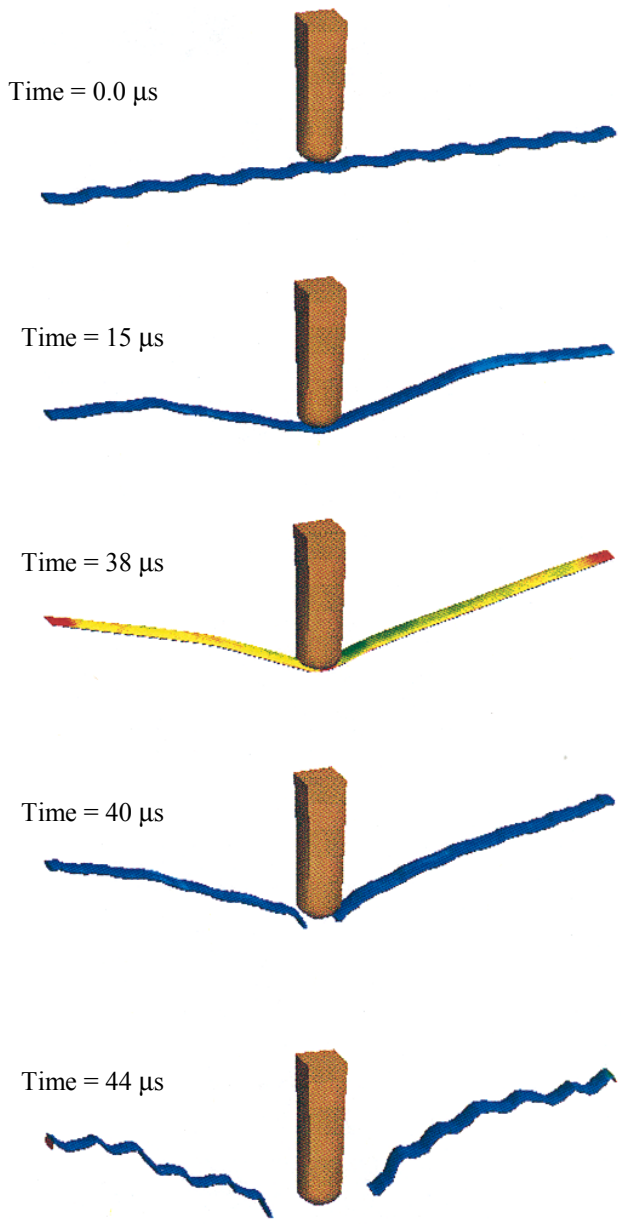

FIGURE 28. SINGLE YARN IMPACTED BY A PROJECTILE AT 80 m/s

The time history of the resisting force of the yarn on the projectile is shown in figure 29. The force is small up to about 25 µs. As the yarn straightens, the force increases. The force reaches a peak of about 1.4 x 10^7 dyne (30 lb).

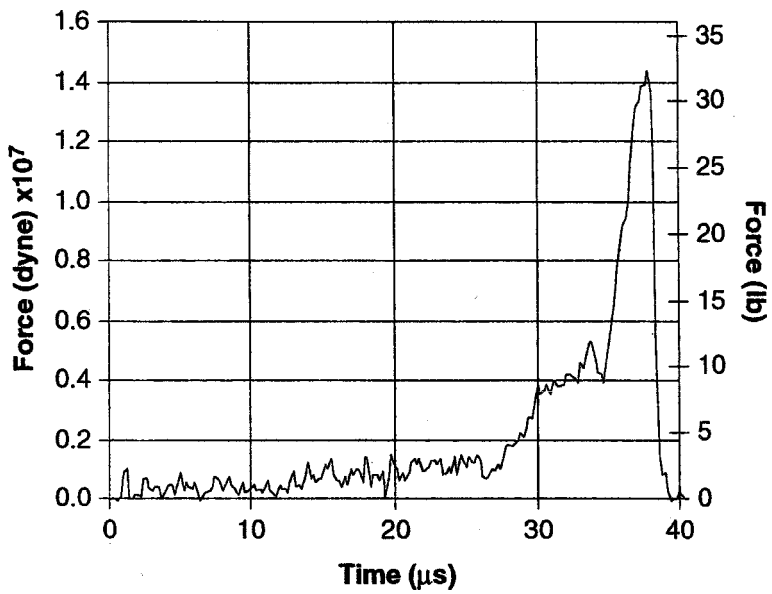

FIGURE 29. RESISTING FORCE OF YARN HIT BY PROJECTILE AT 80 m/s

MODEL DEVELOPMENT PLANS.

Plans for model development are as follows:

1. Verify the fabric model in its current state (brick elements) by implementing it into the DYNA3D code and comparing simulations with the results of the static push tests and yarn pull tests. This model is the detailed model that treats individual yarns and their interaction and captures the yarn mechanics in computing fabric response.

2. Investigate the effect on ballistic performance of the details of the yarn properties and interactions such as interlayer friction, tensile and shear strength of fibers, and strain to failure of fibers. The results of these analyses will help to identify which properties of materials are most important in ballistic performance and thus will help guide the selection of existing materials and help define requirements of new materials. These results will also indicate which material properties must be accounted for in the continuum model (Task 5).

3. Investigate how changes in weave design may lead to improved ballistic performance. The objective here would be to design the weave to involve as many yarns as possible. Yarn kinking and finite element interpenetration are key issues to be solved. Also, the current weave designs are asymmetric: the fill yarns are tighter than the warp yarns.

Current analyses show that this feature causes the impactor to stress the fill fibers well before the warp fibers. Perhaps a more balanced weave design would load the fibers equally and improve the ballistic resistance. Weave design parameters as well as weave pattern will be analyzed to determine which parameters in the weave design have significant effects on ballistic performance.

4. Investigate the effects of boundary conditions on the ballistic performance. Any practical barrier design must rely on the strength of supports to develop the strength of the fibers. For implementation in an aircraft, the existing structural members may be used as a reaction frame. The model will be developed to handle a range of boundary conditions and perform analyses to identify schemes for determining how the existing frame could be used to react with the barrier loads or help design strategies to enhance the strength of the supports with a minimum of added weight.

5. Develop a continuum model for fabric. In order to perform calculations for many multiple layers of fabric economically, a continuum model for the woven fabric is needed that captures the effects of the fabric details but does not model them explicitly. The fabric model will use shell elements and be similar to existing continuum models for computing damage response in composites. The results of our detailed fabric model and our experiments will be used to identify the important response and damage mechanisms and to calibrate the model for single-layer fabrics. The model should be applicable to multiple fabric layers and lay-ups of different design and orientation and would be implementable into DYNA3D as part of the design toolbox. Development of a numerically robust working model for fabrics under impact and penetration loads is a formidable undertaking.